Block Diagram Model of Lathe Machine

M EBRAHIMI, W MOUGHITH AND J VICTORY

School of Engineering
University of Bradford, West Yorkshire, UK

Abstract: This paper presents a computer aided method for the analyses and simulation of a non-linear mathematical model of a CNC Lathe machine tool. The derived model consist of the controller, axis drive and the spindle drive of a CNC turning machine and their connection through the cutting process. The overall model uses a modular multi-model approach to prototype the machine tool and its process.

Keywords: Block-diagram, Lathes, modelling, simulation, dynamic

1 Introduction

The role of virtual prototyping in design, optimization and product development is crucial giving knowledge of cutting forces in the computer modeling and design of the lathe machines. The computer aided analysis generating the cutting forces has been developed by many researchers in the past but these models are either based on mechanistic approaches, which are highly complicated and labour intensive or on statistical methods. There is clearly a need for a simplistic approach, which simulates the dynamic response of the cutting process. The output of the model then can be used as inputs to other CAD packages such as finite element or multi-body dynamic for the structural analysis of the machine. The overall model then can result in a virtual prototyping environment for design optimization. The analysis of the cutting forces can reveal valuable information about the machine tool structure. This is because the cutting process is the one relationship of the whole machine tool dynamic which closes the loop between the axis feed subsystem and the spindle subsystem (Martin and Ebrahimi, 1999). Also it is the cutting process that affects the control of the servo-mechanism, generating the disturbance torque on the feed and the spindle motors.

The turning process has been investigated by many researchers. Mackinnon *et al.* (1986) developed a method of wear estimation for carbide tools using multi-component force measurements for the purpose of tool condition monitoring during adaptively controlled metal cutting on a turret lathe. Dan and Mathew (1990) presented a review for cutting force measurements for on-line tool wear and breakage sensing. El Baradie (1991) discussed a closed loop system with two main elements representing the machine tool structure and the cutting process to develop a generalized statistical theory of chatter to predict a threshold of stability in terms of mean values. Balkrishna and Yung (1999) presented a model of the dynamic cutting force process for the three-dimensional or oblique turning operations. They linked the mechanistic force model to a tool-workpiece-vibration model to predict the dynamic cutting forces. Wen-Hong *et al.* (2001) presented a technique for precision turning of shafts on CNC centre lathes. The precision finish operation was delivered by a piezo-electric based fast tool servo mounted on the same CNC lathe's turret. A sliding mode controller compensates the cutting force disturbances and keeps the tool tip at the desired location within the measurement sensor resolution. Axinte *et al.* (2001) proposed a procedure for the evaluation of those uncertainty components of a single cutting force measurement, which are related to the dynamometer calibration and the cutting process itself. Stein (2002) proposed a cutting force monitoring approach based on the spindle motor current and speed as well as a model relating these measurements to the cutting force.

The non-linear nature of cutting processes makes it impossible to be represented as a simple mathematical function in these CAD packages. Therefore, in this paper, a spindle drive system of a CNC turning machine is modeled and analyzed in physical terms introducing a model of turning cutting processes and interactions.

2 Spindle Drive System

The main components of the turning machine are illustrated in figure 1. The spindle axis drive generates a rotary motion of the workpiece. The *X*-axis drive system, which is not presented in this paper, is mainly used to

develop a longitudinal motion of the table over the slide-ways.

The spindle drive system comprises a DC motor connected to a gearbox, which transfers the motion to the spindle shaft using a belt and pulley mechanism. The input to the DC motor is a controlled voltage V_{SM}, which is supplied from a velocity loop. The input to the velocity loop is a command signal V_C.

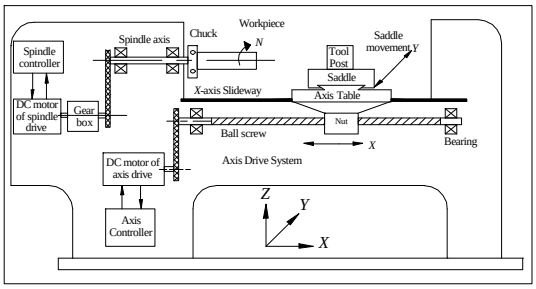

Fig. 1. Schematic representation of the turning machine.

Figure 2 shows a schematic diagram of the velocity loop, which is a pulse width modulated system (*PWM*). The speed regulator is a proportional plus integral controller. The power control loop has a current feed back I_S through a sensor with a gain, K_N. Figure 3 illustrates the block diagram model of the velocity loop (Martain and Ebrahimi, 1999). Where, *s* is the Laplace operator. The first order lag is due to the dynamics of *PWM* (Gross, 1983).

$$G_{PWM} = \frac{1}{K_{PWM}\, s + 1} \qquad (1)$$

where, K_{PWM} is the time constant of G_{PWM}.

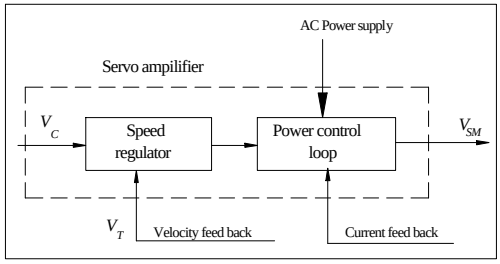

Fig.2. Schematic diagram of the velocity loop

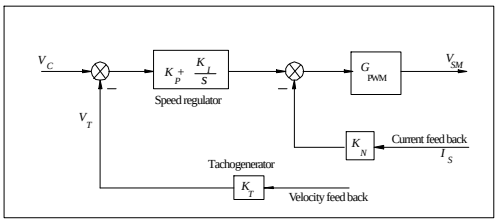

Fig. 3. Block diagram model of the velocity loop

The DC motor circuit and the block diagram model of the electrical part are shown in figure 4. where, *R* and *L* are the resistance and inductance of the armature windings, respectively.

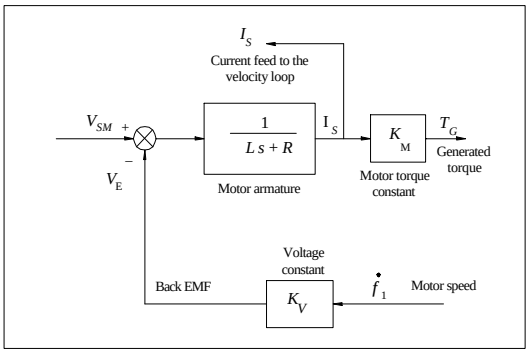

Fig. 4. Block diagram of the spindle motor

Figure 5 shows the free body diagram of the spindle axis drive system.

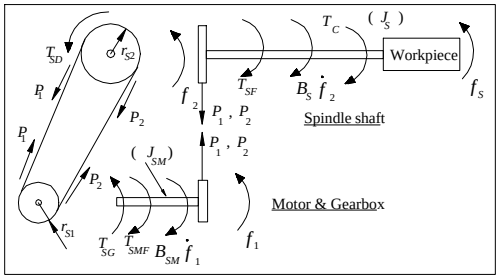

Fig. 5. Spindle drive system free body diagram

where, B_{SM} is the lumped coefficient of the viscous friction in the motor, gearbox, spindle, motor pulley and bearings, B_S is the lumped coefficient of the viscous friction for the spindle bearings and pulley. Also, J_{SM} is the lumped moment of inertia of the spindle motor, gearbox, and pulley and J_S is the lumped moment of inertia of the spindle, pulley, and workpiece. T_{SMF} is the coulomb friction of the spindle motor and gearbox. T_{SF} is the coulomb friction of the spindle shaft bearings. $\dot{f}_1$ and $\dot{f}_2$ represent the spindle motor pulley and spindle axis pulley angular speeds, respectively. P_1 and P_2 are the forces on the tight and slack toothed belt, respectively. T_{SG} is the gross torque generated by the spindle motor armature. T_C is the cutting torque generated by the cutting process. $B_S\ \dot{f}_1$ and $B_S\ \dot{f}_2$ are the resistance torques due to viscous friction in the spindle motor and the spindle shaft, respectively. T_{SD} is the spindle drive torque exerted at the spindle pulley to overcome the cutting torque and friction torque.

3 Equations of Motion

The coulomb friction of the spindle motor and gearbox T_{SMF} are ignored in the beginning to simplify the equations of motion for the motor pulley, which is given below.

$$T_{SG} - (P_1 - P_2) r_{S1} - B_{SM} \dot{f}_1 = J_{SM} \ddot{f}_1 \quad (2)$$

Taking Laplace transformation,

$$T_{SG} - (P_1 - P_2) r_{S1} - B_{SM}\, s\, f_1 = J_{SM}\, s^2\, f_1 \quad (3)$$

where, r_{S1} is the motor pulley radius. Assuming there is no longitudinal strain through the drive belt, then

$$f_1 r_{S1} = f_2 r_{S2} \quad (4)$$

$$\Gamma = \frac{r_{S1}}{r_{S2}} \quad (5)$$

$$f_2 = \Gamma f_2 \quad (6)$$

where, r_{S2} is the spindle pulley radius. Γ is the pulley ratio. Figure 6 illustrates the block diagram of the dynamic part of the DC motor, gearbox, and pulley.

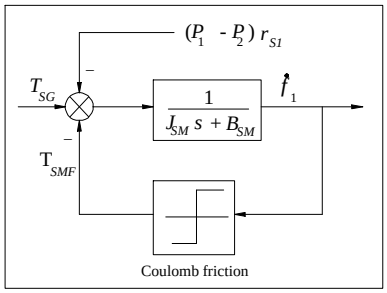

Fig. 6. Block diagram of the dynamic part of the DC motor, gearbox, and its pulley

The angular position of the spindle f_S is less than the angular position of the spindle at the pulley end f_2 due to the elongation in the toothed belt as shown below.

$$f_2 - f_S = df \quad (7)$$

where, df is the angular deflection due to the elongation in the toothed belt assuming that the angular deflection through the spindle shaft is neglected. The elongation in the tight side of the toothed belt is:

$$d_B = (1/K_B)(P_1 - P_0) \quad (8)$$

Where, P_1 is the force in the tight side, P_0 is the pre-load force, and K_B is the linear stiffness of the toothed belt. The reduction in the slack side is equal to the elongation of the tight side of the belt, then:

$$K_B (P_1 - P_0) = K_B (P_0 - P_2) \quad (9)$$

$$(P_1 - P_0) = (P_0 - P_2) \quad (10)$$

$$P_0 = (P_1 + P_2)/2 \quad (11)$$

$$P_1 - P_0 = P_1 - (P_1 + P_2)/2 \quad (12)$$

$$d_B = (1/K_B)(P_1 - P_2)/2 \quad (13)$$

where, P_2 is the force in the slack side of the toothed belt, Assuming that the spindle drive torque T_{SD} causes the toothed belt elongation.

$$T_{SD} = r_{S2} (P_1 - P_2) \quad (14)$$

$$(P_1 - P_2) = T_{SD}/r_{S2} \quad (15)$$

$$d_B = \frac{T_{SD}}{2K_B r_{S2}} \quad (16)$$

The elongation in the toothed belt transfers to a position change in the spindle, df

$$df = d_B / r_{S2} \quad (17)$$

$$df = \frac{T_{SD}}{2 K_B r_{S2}^2} \quad (18)$$

$$df = \frac{T_{SD}}{K_C} \quad (19)$$

$$K_C = 2 K_B r_{S2}^2 \quad (20)$$

where, K_C is the equivalent stiffness in the toothed belt.

2.3 Spindle Drive Shaft

The equation of motion of the spindle drive shaft is

$$-T_C + (P_1 - P_2) r_{S2} - B_S \dot{f}_S = J_S \ddot{f}_S \quad (21)$$

$$-T_C + T_{SD} - B_S\, s\, f_2 = J_S\, s^2\, f_2 \quad (22)$$

where, T_C is the cutting torque acting on the spindle shaft and is related to the tangential force, F_t.

$$T_C = r_{WP}\, F_t \quad (23)$$

where, r_{WP} is the workpiece radius.

Figure 7 represents the block diagram model of the spindle drive system.

4 Turning Cutting Process

The cutting force, *F*, acting on the tool is generated by the engaged part of the cutting edge including the main cutting edge, nose radius, and part of the secondary cutting edge. This force comprises three components as shown in figure 8 (Tlusty, 2000). Where, F_f is the feed force component, F_r is the radial force, and F_t is the tangential force, considered for spindle drive modelling.

There are many variables affecting on the cutting force in turning, some of theses variables are tool geometry, depth of cut, *d*, feed, *f*, cutting speed, V_C which is function of spindle speed, *N*, workpiece hardness, state of lubrication, and tool wear**.** These variables are summarized in the standard equation for the tangential force component as follows (Anon, 1970).

$$F_t = K_{st}\, d^{\,b_t}\; f^{\,a_t} \qquad (24)$$

Where, K_{si} is the specific cutting force. b_t and a_t are constants. The effect of cutting speed V_C on the cutting force can be ignored (Mackinnon *et al.*, 1986). This model when logarithmically transformed becomes:

$$ln\, F_t = ln\, K_{st} + b_t\, ln\, d + a_t\, ln\; f \qquad (25)$$

then, equation (24) can be rewritten as:

$$\hat{y}_{F_t} = b_o + b_1 x_1 + b_2 x_2 \qquad (26)$$

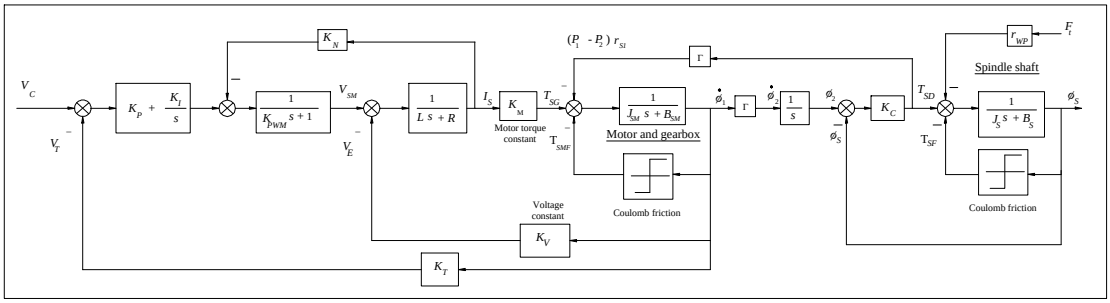

Fig. 7. Block diagram model of the spindle drive system

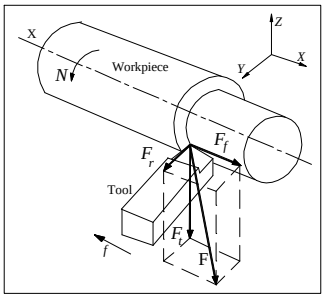

Fig. 8. Cutting force components in turning process

where $\hat{y}_{F_t}$ is the estimated tangential force component and b_o, b_1, and b_2 are the model parameters. x_1 and x_2 are the natural logarithmic value of depth of cut and feed, respectively. Multiple regression analysis estimates these three parameters for the first-order model in equation (25). If there was statistical evidence of lack of fit a second-order or third-order model can be developed. The third-order mathematical model developed will be of the following form.

$$\hat{y}_{F_i} = b_o + b_1 x_1 + b_2 x_2 + b_3 {x_1}^2 + b_4 {x_2}^2 + b_5 {x_1}^3 + b_6 {x_2}^3 + b_7 x_1 x_2 \qquad (27)$$

A second or third-order mathematical model is essential when the true response (tangential force) function is nonlinear or unknown. 32 tests were conducted to identify these cutting model parameters.

A statistical package MINITAB software was used to identify the cutting model parameters, which are b_o, b_1, b_2 , b_3, b_4, b_5, b_6, and b_7. Table 1 shows the tangential force model parameters (coefficients). By investigation table 1, the predictors ${x_1}^2$ and ${x_1}^3$ can be neglected since the *P* value for each predictor is relatively high compared with the other predictors. A further regression is performed after eliminating ${x_1}^2$ and ${x_1}^3$ from the model.

The analysis of variance of the tangential force model is shown in table 2, which shows that the regression model is significant since *P*-value, which is the smallest level of significance that would lead to rejection of the null hypothesis, is 0.00. The value of $F_{0.99;16;10}$ from *F* tables is found to be 4.53. Since $F_{Lack\ of\ fit} < F_{0.99;16;10}$, a lack of fit

is not indicated. The mathematical model of the tangential force is shown below.

$$\hat{y}_{F_t} = 8.2748 + 1.3844\ x_1 + 3.5819\ x_2 + 2.2287\ {x_2}^2 + 0.5329\ {x_2}^3 + 0.2944\ x_1 x_2 \quad (28)$$

Table 1 tangential force model parameters

Predictor	Coefficient	Std. Error	t value	P
Constant	8.2858	0.2944	28.14	0.000
x_1	1.34161	0.07611	17.63	0.000
x_2	3.5819	0.7604	4.71	0.000
${x_1}^2$	-0.02923	0.03743	-0.78	0.443
${x_2}^2$	2.2287	0.6040	3.69	0.001
${X_1}^3$	0.0934	0.1477	0.63	0.533
${x_2}^3$	0.5329	0.1477	3.61	0.001
$x_1 x_2$	0.29442	0.02709	10.87	0.000

Table 2 Analysis of variance of the tangential force model

Source	DF	SS	MS	*F*	*P*
Regression	5	3.7761	2.7552	1676	0.000
Residual Error	26	0.0427	0.0016		
Lack of Fit	10	0.0218	0.0022	1.66	0.176
Pure Error	16	0.0210	0.0013		
Total	31	13.8188			
Model summary	R^2 = 99.7%		R^2_{adj}= 99.6%		

5 Overall Block Diagram

The overall block diagram model of the spindle drive system and turning cutting action is derived by connecting the output of equation 27 after taking the exponential value of $\hat{y}_{F_t}$ of the spindle drive model, as shown in figure 9.

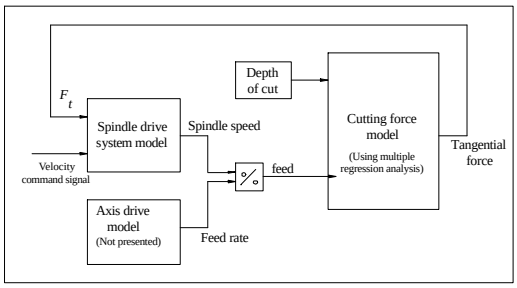

Fig. 9. Schematic block diagram of the spindle drive system model and turning cutting model

6 Simulation

The model has been simulated using MATLAB software. The input to the simulation is the spindle velocity command, feed rate, and depth of cut. The outputs are the motor current, the spindle speed, as shown in figures 10 and 11, respectively.

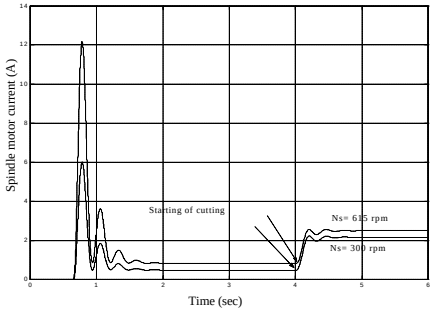

Fig. 10. Simulated spindle motor current

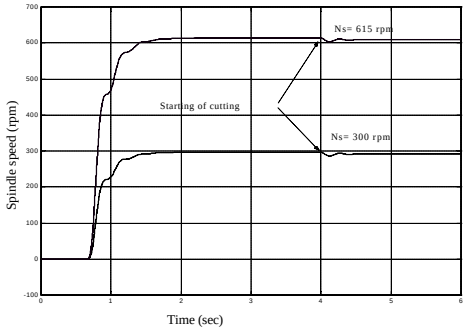

Fig. 11. Simulated spindle speed

Conclusion

Engineers of machine tool design need mathematical models in order to understand the system and its response. The spindle drive model in this paper provides an understanding in showing the linkage between the machine elements and the cutting process. This model can be used in a condition monitoring system for turning processes. In this work the model was produced in a theoretical form and simulated to confirm viability thereafter.

REFERENCES

1. Anon (1970). Adaptive control of machining conditions. MTIRA Research report 35, 8-9.
2. Axinte D.A., W. Belluco, L.D. Chiffre (2001). Evaluation of cutting force uncertainty components in turning", International Journal of Machine Tools & Manufacture, 41, 719-731.
3. Balkrishna C. R., and Y. C. Shin (1999). A Comprehensive dynamic cutting force model for

chatter prediction in turning. International Journal of Machine Tools & Manufacture, 39, 1631-1654.
4. Dan L. and J. Mathew (1990). Tool wear and failure monitoring techniques for turning- A review. International journal of machine tool & Manufacture, 30, 579-598.
5. Ee K.C., A.K. Balaji, P.X.Li, and I.S. Jawahir (2002). Force decomposition model for tool-wear in turning with grooved cutting tool. Wear, 249, 985-994.
6. El-Baradie M.A. (1991). Statistical theory of machine tool stability. Proc. Instn. Mech. Engrs. IMechE, 195-206.
7. Groos, H. (1983). *Electrical Feed Drives for Machine Tools.* John Wiley.
8. Martin,K.F., M. Ebrahimi (July 1999). Modelling and simulation of the milling action. Proc. Instn Mech Engrs, 213, part B, 539-554.
9. Mackinnon R., G.E. Wilson, and A.J. Wilkinson (1986). Tool condition monitoring using multi-component force systems. Matador conference, 317-324.
10. Tlusty, G (2000). *Manufacturing Processes and Equipment*, Prentice hall, Inc., New Jersey
11. Wen-Hong Z., M.B. Jun, and Y. Altintas (2001). A fast tool servo design for precision of shafts on conventional CNC lathes", International Journal of Machine Tools & Manufacture, 41, 953-965.